Sensors & Transducers, Vol. 258, Issue 4, July 2022, pp. 18-24

Sensors & Transducers
Published by IFSA Publishing, S. L., 2022
http://www.sensorsportal.com

High-speed Wavelength Division Multiplexing Transmission over SI-Polymer Fibers

[1, *] Ulrich H. P. Fischer and [2] Mladen Jóncic
[1] Harz University of Applied Sciences, Friedrichstr. 57, 38855 Wernigerode, Germany
[2] Volkswagen AG, 38518 Gifhorn, Germany
[1] Tel.: +49-(0)3943-659351 fax: +49-(0)3943-659399
E-mail: ufischer@hs-harz.de

Received: 10 June 2022 /Accepted: 17 July 2022 /Published: 29 July 2022

Abstract: In short-range communication 1 mm PMMA SI-POF established itself as a reasonable alternative to the traditional data communication media such as glass fibers, copper cables and wireless systems. Due to multiple advantages such as a large core diameter, tolerance to fiber facet damages and low installation costs, the SI-POF is already applied in industrial automation, automotive industry and in-house/office networks. The commercial systems with SI-POF use a single channel for data transmission. Utilization of several optical carriers for parallel transmission of data channels over a single fiber, known as WDM, represents another alternative to increase the capacity of SI-POF link. To experimentally demonstrate the feasibility and potential of a high-speed POF WDM concept, a four-channel data transmission setup was realized. In addition, the record 14.77 Gb/s data rates employing the offline-processed DMT modulation were demonstrated over 50 m SI-POF, respectively, at the BER=10^{-3}. Compared to the fastest single-wavelength systems, two times higher transmission capacity was achieved

Keywords: Polymeric optical fibers, WDM transmission, WDM Multiplex, WDM Demultiplex, WDM over POF.

1. Introduction

Having its origin in the 1960's as well as the silica glass fiber, the polymer optical fiber (POF) stayed long in the shadow of the huge development and success of glass fiber communications. However, the advances in POF technology and the growing need for high-speed short-range communication networks make POF nowadays gain more and more in importance. The key advantage of POF is a large core diameter. It makes POF tolerant to the fiber facet damages and relaxes the alignment tolerances, thus also reducing the installation costs.

Furthermore, POF is pliable, durable, and inexpensive, offers small weight and short bend radius, allows easy installation, simple termination and quick troubleshooting, and also provides the immunity to electromagnetic interference. Due to its diverse advantages, in short-range applications POF established itself as a reasonable alternative to the traditional data communication media such as glass fibers, copper cables and wireless systems (see Table 1).

Today, POF is produced with different core materials, core diameters and index profiles. Two major POF types are made of polymethyl methacrylate (PMMA) and perfluorinated (PF) materials. The parameters of the common PMMA and PF POFs are specified in the IEC Standard 60793-2-40, which defines eight different POF classes [1].

Table 1. Comparison of different transmission media; Characteristics very bad (--) to very good (++).

Transmission medium	Data rate	Distance	Safety	Cost	Handling	Installation	Total
Twisted pair cable	+	0	0	++	-	0	**2+**
Coaxial cable	0	0	0	+	0	0	**1+**
Glass fiber	++	++	++	--	--	-	**1+**
Polymer fiber	0	-	++	+	+	+	**4+**
Wireless	--	-	--	++	++	++	**1+**
Powerline	-	-	--	+	+	++	**0**

The PMMA POF is produced with both step-index (SI) and graded-index (GI) profile, whereas the PF POF offers only GI profile. The GI profile of the core ensures high modal bandwidth exceeding 1.5 GHz × 100 m for the PMMA POF and 300 MHz × 1 km for the PF POF. However, the implementation of the PMMA GI-POF is confined to 500-680 nm wavelength range due to the high optical attenuation at other wavelengths (> 400 dB/km). The PF GI-POF is best suited for use in the infrared region, e.g. in the first (850 nm) and the second (1300 nm) optical window, where of-the-shelf components developed for multimode glass fibers are available. In contrast, the PMMA SI-POF suffers from intermodal dispersion limiting the bandwidth-length product to around 50 MHz × 100 m (see [2]), but also provides several attenuation windows in the visible spectrum (400-700 nm). Due to its advantages over the other POF types such as technological maturity, ease and cost of production and high numerical aperture (NA), the standard 1 mm PMMA SI-POF (POF class A4a.2 according to IEC 60793-2-40) is the best known and by far the most widely employed type of POF. This is also the fiber the paper concentrates on. Throughout the work the terms SI-POF and POF will be equally used to address this fiber type. A comprehensive overview on various POFs is given in [3].

Three major application sectors of SI-POF data communication technology are industrial automation, automotive industry and in-house/office networks.

The commercial systems with SI-POF use a single channel for data transmission. However, the data carrying capacity of SI-POF is impaired by strong inter-modal dispersion and high optical attenuation. Over the last few years various concepts to overcome the bandwidth limitation of SI-POF have been successfully demonstrated, including optimization of the optoelectronic components and implementation of the digital signal processing techniques. The bus systems such as Profibus (1.5 Mbit/s, 60 m) and industrial Fast Ethernet (100 Mbit/s, 50 m) are typical applications and since 2013 also the Gigabit Ethernet transceivers (1 Gb/s) are available on the market enabling the transmission of broadband services over 50 m SI-POF [4].

1.1. Capacity Extension by WDM Technology

The most frequently mentioned motivation for POF WDM is to increase the transmission capacity of SI-POF link compared to the single-wavelength systems.

Complying with any of the hitherto developments, utilization of several optical carriers for parallel transmission of data channels over a single fiber represents another alternative to increase the transmission capacity of SI-POF. The technique is well known as wavelength division multiplexing (WDM). In glass fiber communications WDM has been firmly established for more than two decades and represents the key technology in modern high-capacity optical networks with the distances ranging from several thousand down to ~100 km [5], [6], [7].

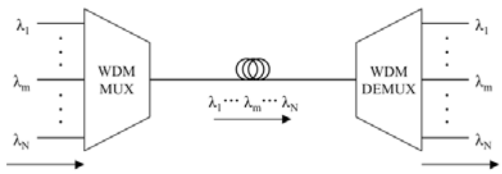

Fig. 1. Principle of WDM: MUX – Multiplexer, DEMUX – Demultiplexer.

The principle of WDM is shown in Fig. 1. Since different wavelengths λ_1–λ_N do not interfere with each other in a linear medium, they can be used to simultaneously carry the data signals over a single fiber. Two components are essential for WDM, a wavelength multiplexer and demultiplexer. The multiplexer combines the signals at different wavelengths, coming from different transmitters, onto a single fiber. On the opposite side of the optical link the demultiplexer performs an inverse function, separating the wavelength channels to be detected by separate receivers. Because of e.g. interchannel crosstalk, the demultiplexer is more often considered in fiber optics. Therefore, this thesis concentrates on the demultiplexing function without loss of generality for the multiplexing operation.

The existing WDM components developed for single-mode glass fibers in the infrared region, such as Mach-Zehnder interferometers, arrayed waveguide gratings or fiber Bragg gratings, cannot be reused for a highly multimode SI-POF. On the other hand, the operating principles of demultiplexers based on thin-film interference filters and on a diffraction grating can be applied for POF. In spite of some other demultiplexing solutions (e.g. employing dispersion prisms), these two demultiplexing techniques have been recognized as the most promising for SI-POF. However, because of the difference in the operating wavelength range, fiber diameter, NA, etc. compared to the glass fibers, such demultiplexers must be newly designed for SI-POF communication. The paper concentrates on the demultiplexing techniques employing thin-film interference filters and a concave diffraction grating.

In the early attempts, the LED-based POF systems exploiting WDM technology could not provide sufficient capacity [8], [9]. Only recently, supported by the advance in the visible laser diode technology, the record-breaking POF WDM transmission experiments, including the work of the author, were performed [10-12].

2. POF Multiplexer

As mentioned on Chapter 1.1, the multiplexer can be realised in a simpler way than the demultiplexer. The principal idea of a small device is shown in Fig. 2. A FC/PC connector was used to combine 4 incoming small POFs with diameters of 400 µm in a plug and couple this plug in a connector to a 980/1000 µm SI-POF. The NA of the incoming 400µm POFs is the same as the SI-POF of 0.5. Since the numerical aperture of both fiber types is identical, the losses in the connection from connector to connector are very low.

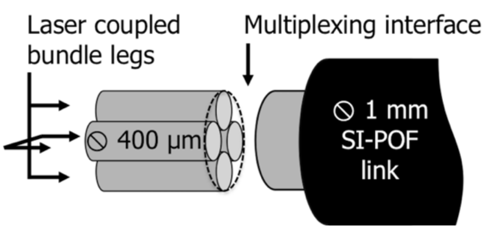

Fig. 2 Principale of operation.

In addition, the fibers are butt-coupled at the end face, so that losses due to reflection at air gaps are avoided. The Performance of the device has measured insertion losses between 3.3 dB – 5.5 dB. The losses are based on launching coupling loss between the two fiber types. Additionally, losses are coming from the attenuation of bundle leg and from the multiplexing interface.

A photograph and the technical setup is shown in Fig. 3. A FC/PC connector combines the two FC/PC plugs with the different fiber types and a simple setup of the optical multiplexer for POF was realised.

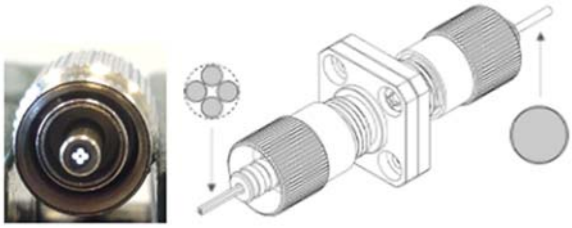

Fig. 3. Practical realisation in a FC/PC connector.

3. For Channel Demultiplexer

The demultiplexer was realized with the components from LINOS Microbench series and was installed on a vibration suppressing optical table. The principle of operation of a four-channel demultiplexer with two-stage configuration is shown in shown in Fig. 4. A 4-rod construction system supported with the mounting holders was used to bring together the Microbench mechanical components holding the fibers and bulk optical elements. The ingoing and the outgoing fibers, which were terminated with SMA connectors, were mounted over SMA fiber adapters into XYZ fine adjustment units. The units provided a travel range of ±1 mm in the x- and y-direction, and when anchored to the 4-rod system allowed a travel of 5 mm along the optical axis (z-direction). The aspheric lenses were mounted in XY precision translation stages having a travel range of ±1 mm along the x- and y-direction. The collimating lens with 25 mm mounting diameter was directly mounted in the stage, whereas the focusing lenses with a smaller mounting diameter were mounted over reduction inserts. In each of the output ports the bandpass interference filter was mounted in the XY precision translation stage in front of the aspheric lens. The dichroic mirrors are glued to an adjustable mirror insert was positioned within a beam splitter cube over a rotation adjustment for cube insert.

In Fig. 5 a photograph of the mechanical and optical setup is depicted. The first stage of the demultiplexer, represented by a dichroic mirror that follows directly after the collimating lens, split the incident spectrum into two spectral bands. The separation of the individual wavelength channels was then performed within the second stage of the demultiplexer.

Accordingly, the demultiplexer setup allowed very precise positioning and alignment of the fiber end faces, lenses and dichroic mirrors. The available degrees of freedom can be summarized as follows:

- End faces of the ingoing and the outgoing fibers: x-, y- and z-direction translation;
- Collimating and focusing lenses: x- and y-direction translation;

- Dichroic mirrors: rotation and tip/tilt (when applied together tip and tilt result in translation along the direction perpendicular to the incoming optical axis).

To measure the transfer function of the demultiplexer, a Yokogawa AQ4305 white light source followed by a cylinder mode mixer according to JIS 6863 provided a wide spectral range (400-700 nm) to the input of the demultiplexer. The spectral responses of the channels were recorded by a Yokogawa AQ-6315A optical spectrum analyser.

Table 2. Basic parameters of four channel multiplexer.

Output port	1	2	3	4
Center wavelength [nm]	404.9	450.1	528.3	646.4
3 dB passband bandwidth [nm]	9.4	9.3	41.6	47.6
Minimum IL [dB]	5.66	4.55	3.47	3.19
IL uniformity [dB]	2.47			
(Non)adjacent channel isolation [dB]	> 30			

The corresponding transfer function is shown in Fig. 6. The basic parameters of the demultiplexer are given in Table 2. The measurement results for the four-channel demultiplexer with two-stage configuration were presented at the International Conference on Plastic Optical Fibers (ICPOF) 2013 [13]. To comply with all other measurements shown in this chapter, which were performed two years thereafter, the demultiplexer setup was assembled and characterized again. While preserving the same principal behaviour of the spectral response, the minimum IL in the output ports 1 to 4 was 6.15 dB, 5.44 dB, 4.21 dB and 3.85 dB respectively. Those were by 0.49 dB, 0.89 dB, 0.74 dB and 0.66 dB higher values than those reported in [14].

The device is well suited for implementation in high-speed POF WDM transmission experiments.

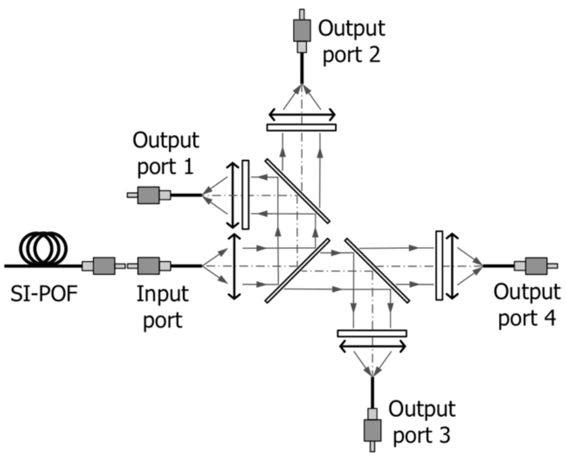

Fig. 4. Principle setup of a four-Channel Demultiplexer with Interference Filters.

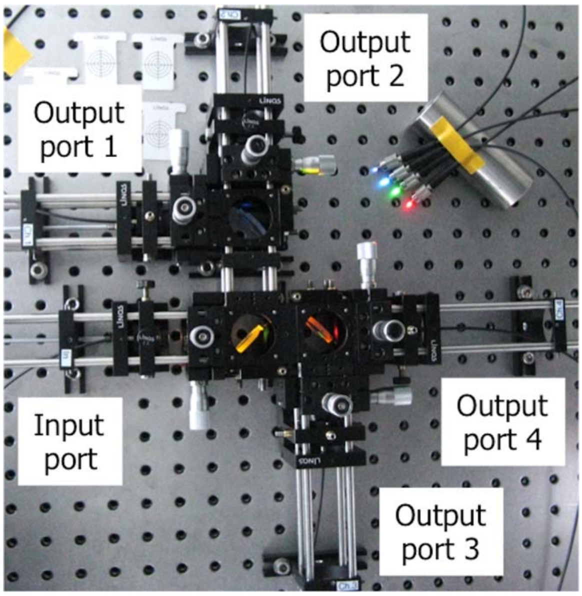

Fig. 5. Realisation of the 4 Channel Demultiplexer.

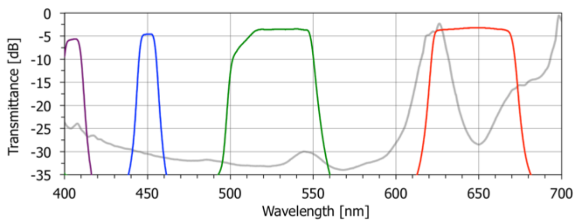

Fig. 6. Transmittance of the Demultiplexer.

4. Four-channel POF WDM Transmission Experiments

The data transmission setup is shown in Fig. 7. It comprised an Agilent N4903A bit error rate tester (BERT), four butt-coupled edge-emitting laser diodes, multiplexing POF coupler, 50/100 m SI-POF link, interference-based POF demultiplexer, optical receivers and Agilent 86100B sampling oscilloscope.

To combine the optical signals (MUX) with different wavelengths onto the SI-POF link, a Comcore 4×1 fused POF coupler was used. For direct launching with 405 nm (DL-5146-101S), 450 nm, 515 nm and 639 nm laser diodes, the IL between any of four input (laser coupled) ports and the output port was 8-9 dB.

The experimental setup for the measurements employing the offline-processed DMT modulation is shown in Fig. 7. It comprised the four-channel Agilent M8190A AWG, four butt-coupled edge-emitting laser diodes, four-legged multiplexing POF bundle, SI-POF link of two different lengths (50, 100m), interference-based POF demultiplexer, optical receivers, four-channel Agilent DSA91604A real-time oscilloscope and computer with a software for offline signal processing.

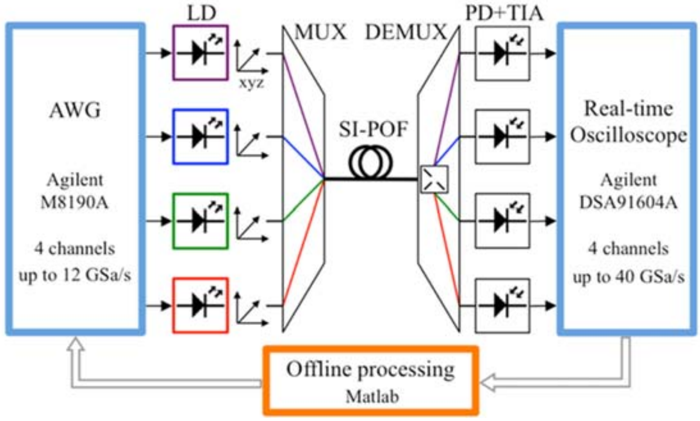

Fig. 7. Experimental setup for the measurements employing offline-processes DMT modulation: LD – laser diode; MUX – multiplexer; DEMUX – demultiplexer; PD – photodiode; TIA – transimpedance amplifier.

The photograph of the electrical and optical setup can be seen in in Fig. 8. Here the following components are depicted:

1- DMT AWG;
2- RF amplifier for LD modulation;
3- RF – Y-Connectors for the LDs;
4- LD Cooler;
5- LD Cooler controller slot;
6- LD Cooler input device hub Tektronix;
7- Multiplexer;
8- 50m Si-POF;
9- Demultiplexer;
10- High speed optical Receiver;
11- Real time Oscilloscope;
12- Optical integration sphere;
13- Optical power meter.

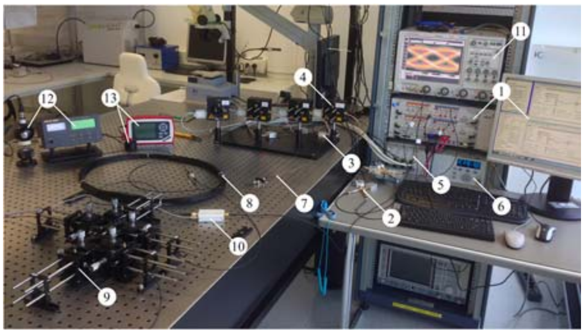

Fig. 8. Experimental Data transmission setup.

4.1. Experimental Results

To estimate the quality of the WDM channels and allocate the number of bits per subcarrier, four DMT pilot signals with 256 subcarriers, each loaded with 16-QAM, were simultaneously transmitted over four channels. In 50 m and 100 m experiments the bandwidth occupied by the pilot signals was initially set to 1 GHz and 500 MHz respectively.

To decorrelate the signals that modulated the laser diodes, an additional delay of 10 ns between the channels was introduced in the AWG. The received signals were demodulated and used to evaluate the SNR per subchannel. For the case the SNR in the highest subchannels was high enough to allow transmission of additional bits at even higher subcarrier frequencies, the bandwidth of the pilot signal was accordingly increased and the measurement was repeated.

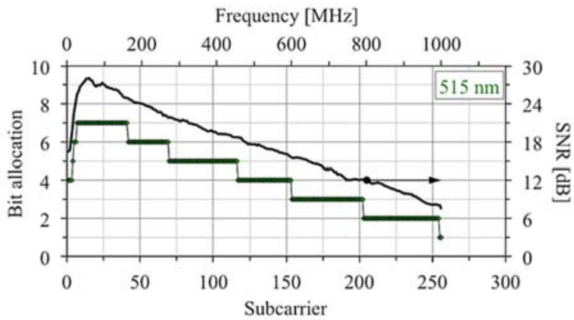

Fig. 9. Measured example SNR per subcarrier before bit-loading (solid black curve) and bit-loading scheme obtained on the basis of Chow's rate adaptive bit-loading algorithm (curve with markers) for the 515 nm channel in 50 m POF experiment.

The evaluated SNR per subchannel was used as input to the Chow's rate adaptive bit-loading algorithm that computed the appropriate bit-loading scheme and power allocation per subchannel [15]. Based on the obtained bit and power allocations across the subcarriers, the real-valued samples of the DMT time signal were pre-computed offline. After that, the DMT samples were loaded into the memory of the AWG and repeatedly played in order to create a continuous-time DMT signal that directly modulated the intensity of the laser diode. The received DMT frames were captured by the oscilloscope for subsequent offline processing that comprised DMT demodulation, SNR evaluation and BER counting.

After deduction of the DMT transmission overhead, the data rates transmitted in the individual WDM channels were 3.26 Gb/s (405 nm channel), 3.90 Gb/s (450 nm channel), 4.08 Gb/s (515 nm channel) and 3.53 Gb/s (639 nm channel). The total averaged BER in each channel was 10^{-3} allowing the FEC with 7 % overhead. Therefore, an aggregate bit rate of 14.77 Gb/s achieved at the BER=10^{-3} corresponded to 13.8 Gb/s information bits at the BER<10^{-9}. A measured example of the bandwidth of the subcarrier behavior of the green Channel at 515nm is depicted in Fig. 9.

In Fig. 10 the measured symbol bits are depicted. The measurement represents a superimposed constellation diagram of the subcarrier group modulated with 4-QAM (182nd to 185th and 191st to 232nd subcarrier). An averaged received SNR for the subcarrier groups modulated with 256-QAM and 4-QAM, obtained from the measurement data from Fig. 5.16a, equals 29.22 dB and 9.76 dB respectively.

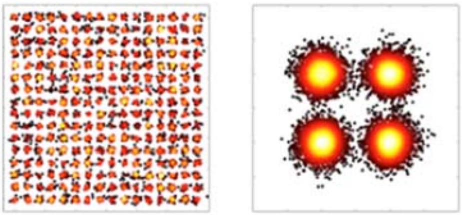

Fig. 10. Measured QAM signals with 256/8bits/symbol (left) and 4 QAM with 2bit/symbol (right).

Table 3. Comprehension of measured data rates for 4 channels via 50m and 100m SI-POF.

WDM channel	50 m	100 m
Violet 405 nm	3.26 Gb/s	1.34 Gb/s
Blue 450 nm	3.90 Gb/s	2.09 Gb/s
Green 520 nm	4.08 Gb/s	2.84 Gb/s
Red 656 nm	3.53 Gb/s	1.99 Gb/s
Total (BER=10^{-3})	**14.77 Gb/s**	**8.26 Gb/s**
Error free (with FEC)	**13.80 Gb/s**	**7.72 Gb/s**

Therefore, an aggregate bit rate of 14.77 Gb/s achieved at the BER=10^{-3} corresponded to 13.8 Gb/s information bits at the BER<10^{-9}. All data rates measured for the four transmission channels via 50m and 100m SI POF are listed in Table 3. The realized system provided 2.3 times more capacity than the fastest 50 m single-wavelength system known from literature, which operated at 650 nm [16].

5. Conclusions

In this work it was shown, that WDM transmission over POF realised a huge extension of overall data rates within one fiber over 50 m. The 14.77 Gb/s data transmission based on the offline-processed DMT modulation was demonstrated over 50 m SI-POF at the BER=10^{-3}. That is the second highest transmission capacity ever achieved over 50 m SI-POF.

Enabling higher WDM data rates, it will be possible to reach data rates for POF WDM Systems with up to 40 Gbit/s with 16 WDM channels.

Acknowledgements

We thank the German Federal Ministry of Research (BMBF) for support this work under project HOPE (**H**igh speed **O**ptical transmission over **P**olym**E**r fibers)

References

[1]. T. Specification, IEC09, and T. Specification, TS 105 175-1 - V1.1.1 - Access, Terminals, Transmission and Multiplexing (ATTM); Plastic Optical Fibre System Specifications for 100 Mbit/s and 1 Gbit/s, Vol. 1, pp. 1–16, 2010.

[2]. J. Zubia and J. Arrue, Plastic Optical Fibers: An Introduction to Their Technological Processes and Applications, *Opt. Fiber Technol.*, Vol. 7, No. 2, 2001, pp. 101–140.

[3]. O. Ziemann, J. Krauser, P. E. Zamzow, POF Handbook: Optical Short Range Transmission Systems., *Springer Verlag*, Berlin Heidelberg, 2008.

[4]. K. L. Johnson, W. Hogan, M. M. Dummer, and C. Steidl, Advances in High-Speed Red Vcsel Performance, *Adv. Opt. Technol.*, Vol. 2012, 2012, pp. 5–10.

[5]. B. Mukherjee, WDM optical communication networks: progress and challenges, *Sel. Areas Commun. IEEE J.*, Vol. 18, No. 10, 2000, pp. 1810–1824.

[6]. S. V. Kartalopoulos, DWDM: Networks, Devices, and Technology, *Wiley-IEEE Press*, 2002.

[7]. H.-J. Thiele and M. Nebeling, Coarse wavelength division multiplexing: technologies and applications, *CRC Press*, 2007.

[8]. P. J. Pinzón, I. Pérez, and C. Vázquez, Visible WDM System for Real-Time Multi-Gb/s Bidirectional Transmission over 50-m SI-POF, *IEEE Photonics Technol. Lett.*, Vol. 28, No. 15, 2016, pp. 1696 – 1699.

[9]. X. Li *et al.*, 11 Gb/s WDM transmission over SI-POF using violet, blue and green μlEDs, in *Proceedings of the Optical Fiber Communications Conference and Exhibition (OFC 2016)*, 2016, paper Tu2C.5.

[10]. R. Kruglov, J. Vinogradov, S. Loquai, O. Ziemann, C.-A. Bunge, T. Hager, 21.4 Gb/s discrete multitone transmission over 50-m SI-POF employing 6-channel WDM, in in *Proceedings of the OFC/NFOEC*, 2014, paper Th2A.2.

[11]. M. Joncic *et al.*, Four-Channel WDM Transmission Over 50-m SI-POF at 14.77 Gb/s Using DMT Modulation, *Photonics Technol. Lett. IEEE2*, Vol. 26, No. 13, 2014, pp. 1328–1331.

[12]. I. Yahav, N. Sheffi, Y. Biofcic, and D. Sadot, Multi-Gigabit Spatial-Division Multiplexing Transmission over Multicore Plastic Optical Fiber, *J. Light. Technol.*, Vol. 39, No. 8, Apr. 2021, pp. 2296–2304.

[13]. U. F.-H. [Joncic13c] M. Jončić, M. Haupt, Development status of a four-channel CWDM system for Multi-Gbit/s in-house data communication via SI-POF, *20. ITG-Fachtagung Kommun.*, p. 6, 2013.

[14]. U. H. P. P. Fischer, S. Höll, M. Haupt, and M. Joncic, Integrated Optical Demultiplexer for WDM Communication Systems, in *Proceedings of the 6th Electronics System-Integration Technology Conference*, 2016, p. 155.

[15]. P. S. Chow, J. M. Cioffi, and J. A. C. Bingham, A practical discrete multitone transceiver loading algorithm for data transmission over spectrally shaped channels, *IEEE Trans. Commun.*, Vol. 43, No. 2, 1995, pp. 773–775.

[16]. J. Vinogradov, R. Kruglov, S. Loquai, O. Ziemann, Multi gigabit transmission with blue, green and red laser diodes, in *Proceedings of the 20th International Conference on Plastic Optical Fibers*, 2011, pp. 467–470.
